

## Novel Regulation of Smad3 Oligomerization and DNA Binding by Its Linker Domain<sup>†</sup>

Eleftheria Vasilaki,<sup>‡</sup> Manos Siderakis,<sup>‡</sup> Paraskevi Papakosta, Konstantina Skourti-Stathaki, Sofia Mavridou, and Dimitris Kardassis\*

*Department of Basic Sciences, University of Crete Medical School and Institute of Molecular Biology and Biotechnology, Foundation of Research and Technology-Hellas, Heraklion 71003, Greece.<sup>‡</sup>These authors contributed equally to this work*

*Received March 31, 2009; Revised Manuscript Received June 30, 2009*

**ABSTRACT:** Smad proteins are key effectors of the transforming growth factor  $\beta$  (TGF $\beta$ ) signaling pathway in mammalian cells. Smads are composed of two highly structured and conserved domains called Mad homology 1 (MH1) and 2 (MH2), which are linked together by a nonconserved linker region. The recent identification of phosphorylation sites and binding sites for ubiquitin ligases in the linker regions of TGF $\beta$  and bone morphogenetic protein (BMP) receptor-regulated Smads suggested that the linker may contribute to the regulation of Smad function by facilitating cross-talks with other signaling pathways. In the present study, we have generated and characterized novel Smad3 mutants bearing individual substitutions of conserved and nonconserved amino acid residues within a previously described transcriptionally active linker fragment. Our analysis showed that the conserved linker amino acids glutamine 222 and proline 229 play important roles in Smad functions such as homo- and hetero-oligomerization, nuclear accumulation in response to TGF $\beta$  stimulation, and DNA binding. Furthermore, a Smad3 mutant bearing a substitution of the nonconserved amino acid asparagine 218 to alanine displayed enhanced transactivation potential relative to wild type Smad3. Finally, Smad3 P229A inhibited TGF $\beta$  signaling when overexpressed in mammalian cells. In conclusion, our data are in line with previous studies supporting an important regulatory role of the linker region of Smads in their function as key transducers of TGF $\beta$  signaling.

Transforming growth factor  $\beta$  (TGF- $\beta$ <sup>1</sup>) is the prototype member of a large, evolutionarily conserved, superfamily of cytokines that, in addition to TGF $\beta$ , includes the activins, the bone morphogenetic proteins (BMPs), and the growth and differentiation factors (GDFs) among others (1, 2). TGF $\beta$  controls various processes during embryogenesis such as growth and differentiation, epithelial to mesenchymal transition (EMT), and angiogenesis, and is an important homeostatic regulator in the adult organism (1, 2). Because of its cytostatic program, which involves the positive or negative regulation of the transcription of genes such as p21<sup>CDKN1A</sup>, p15<sup>CDKN2B</sup>, c-myc, and Id (inhibitors of differentiation), TGF $\beta$  is a suppressor of epithelial cell growth (3). However, during the late stages of carcinogenesis and metastasis, TGF $\beta$  acts as a tumor promoter because of its ability to enhance processes such as epithelial to mesenchymal transition, cell motility and invasion, immunosuppression, angiogenesis, and extracellular matrix production (3, 4).

All members of the TGF- $\beta$  superfamily signal via a classical pathway, which consists of a heterotetrameric complex of two type I (T $\beta$ RI) and two type II (T $\beta$ RII) Ser/Thr kinase receptors on the plasma membrane and downstream cytoplasmic effector proteins termed Smads (5–7). TGF- $\beta$  promotes receptor oligomerization which leads to the phosphorylation of the type I TGF $\beta$  receptors by the constitutively active type II receptors. Activated type I receptors (also called ALK5), phosphorylate Smad2 and Smad3 (also called receptor regulated Smads or R-Smads) at their C-terminal SSXS motives (5–7). The R-Smads in turn oligomerize with the common partner Smad4 and rapidly translocate to the nucleus where they bind to the promoters of a large variety of target genes and regulate the levels of their expression in a positive or a negative manner (5–7).

All R-Smads and Smad4 contain two highly conserved domains called MH1 (Mad homology 1) and MH2 at their N- and C-terminal ends, respectively, which are separated by a nonconserved middle linker region (7). The MH1 domain contains a  $\beta$ -hairpin secondary structure which makes contacts with nucleotides of Smad DNA binding elements (SBEs, 5'-CAGAC-3') present in the promoters of TGF $\beta$  target genes (8). The MH1 domain also contains a nuclear localization signal, binding sites for regulatory proteins, and negatively regulates the functions of the MH2 domain (9). The MH2 domain is essential for the interaction of R-Smads with SARA (Smad Anchor for Receptor Activation), their phosphorylation by the type I receptors, their homo- and hetero-oligomerization, and their interaction with regulatory factors in the nucleus such as transcriptional coactivators and corepressors (7). Crystallographic studies of isolated Smad MH2 domains have established that this domain is

<sup>†</sup>This work was funded by a grant from the Hellenic Ministry of Education (Pythagoras II), the Hellenic Ministry of Development (PENED03-688), and by the Institute of Molecular Biology and Biotechnology of Crete.

\*Corresponding author. Laboratory of Biochemistry, Department of Basic Sciences, University of Crete Medical School, Heraklion, Crete, Greece GR-71003. Tel: +30-2810-394549. Fax: +30-2810-394530. E-mail: kardassis@imbb.forth.gr.

<sup>1</sup>Abbreviations: bio, biotinylation; BMP, bone morphogenetic proteins; CA, constitutively active; DBD, DNA binding domain; ERK, extracellular signal-regulated kinase; HEK, human embryonic kidney; MH1, Mad homology 1; p/CAF, p300/CBP associated factor; PAI-1, plasminogen activator inhibitor-1; R-Smads, receptor-regulated Smads; SAD, Smad4 activation domain; SBEs, Smad DNA binding elements; SARA, Smad anchor for receptor activation; T $\beta$ RI, type I TGF $\beta$  receptor; TGF- $\beta$ , transforming growth factor  $\beta$ .

composed of a central  $\beta$ -sandwich core element capped by a three-helical bundle at one end and a loop/helix region at the opposite end (10). Point mutations at highly conserved amino acid residues either in the loop/helix region or the three-helical bundle of the MH2 domain that disrupt Smad4 homo- and hetero-oligomerization have been described in cancer patients (10–12).

The highly conserved MH1 and MH2 domains of R-Smad and Smad4 proteins are linked together by a nonconserved, proline-rich, linker region. It was believed that the linker is just a flexible hinge that facilitates the free movement of the MH1 and MH2 domains. However, the identification of phosphorylation sites for MAP kinases, cyclin dependent kinases, and  $\text{Ca}^{2+}$ /calmodulin kinase II (CaMKII) in the linker regions of R-Smads suggested that the linker may contribute to the regulation of Smad function by facilitating cross-talks with other signaling pathways (13–19). Furthermore, the linker regions of Smad3 and Smad4 were shown to harbor, at their C-terminal ends, a transactivation domain and that an internal deletion of this domain in Smad3 abolished the Smad-mediated transactivation of TGF $\beta$  target promoters (20–22). The linker region also contains binding sites for the ubiquitin ligase Smurf1 (23). Recently, it was shown that a peptidyl-prolyl cis–trans isomerase (PPIase) Pin1 interacted with Smad2 and Smad3 but not Smad4 and that this interaction was enhanced by the phosphorylation of S/T-P motifs in the Smad linker region (24). S/T-P motif phosphorylation also enhanced the interaction of Smad2/3 with Smurf1 or Smurf2, whereas silencing of the Pin1 gene increased the protein levels of endogenous Smad2/3 (23).

In the present study, we have undertaken a mutagenesis analysis of the linker region of Smad3 protein in order to identify novel residues that contribute to its functions. Our findings indicate that amino acid substitutions in this region could influence various Smad functions including interaction with SARA, oligomerization, translocation to the nucleus, DNA binding, and transcriptional activation. Our data are in line with previous studies supporting an important regulatory role of the linker region of Smads in their function as key effectors of TGF $\beta$  signaling in mammalian cells.

## MATERIALS AND METHODS

**Materials.** Dulbecco's modified Eagle's medium (DMEM) and penicillin/streptomycin for cell culture, Dynabeads, Trizol reagent for RNA extraction, Super-Script RNase H-reverse transcriptase, goat antimouse Alexa Fluor 488, and goat anti-rabbit Alexa Fluor 555 were purchased from Invitrogen/Life Technologies (Carlsbad, CA, USA). Fetal bovine serum (FBS) was purchased from BioChrom Laboratories (Terre Haute, IN, USA). Restriction enzymes and modifying enzymes (T4 DNA ligase and calf intestinal alkaline phosphatase) were purchased from Minotech (Heraklion, Greece) or New England Biolabs (Beverly, MA, USA). GoTaq DNA polymerase, dNTPs, the luciferase assay system and Wizard SV gel and PCR cleanup system were purchased from Promega (Madison, WI, USA). Streptavidin-agarose, streptavidin-HRP, and the anti-Flag M2 (F 3165) mouse monoclonal antibody were purchased from Sigma-Aldrich (St Louis, MI, USA). The Super Signal West Pico Chemiluminescent Substrate was purchased from Pierce (Rockford, IL, USA). G-Sepharose beads were purchased from General Electric Health Care (Chalfont St Giles, UK). The mouse anti-GST (B-14) antibody was purchased from Santa Cruz Biotechnology (Santa Cruz, CA, USA). The P-Smad3 and ALK5 antibodies were provided by Dr. Aris Moustakas (Ludwig Institute for Cancer Research, Uppsala, Sweden). The antimouse and antirabbit peroxidase conjugated secondary antibodies were purchased from Chemicon International Inc. (Temecula, CA, USA).

**Plasmids.** Plasmids expressing the wt human Smad3 tagged with the 6myc epitope or fused with the DNA binding domain (DBD) of GAL4 have been described previously (21). The mutants bearing the single amino acid substitutions N218A, Q222A, and P229A in Smad3 were constructed by overlap extension PCR (25). Each amplified fragment corresponding to a particular Smad mutant was cloned at the *Eco*RI and *Not*I sites of either the pCDNA1amp-6Xmyc vector in frame with a 6myc epitope tag or into the pCDNA3-Bio vector in frame with the biotinylation tag and then subcloned into the pBXG1 vector at the *Eco*RI and *Xba*I sites in frame with the DNA binding domain of GAL4. The sequences of all primers used in the PCR

Table 1: Oligonucleotides Used in Mutagenesis, Reverse Transcription PCR (RT-PCR), DNA Affinity Precipitation (DNAP), and Chromatin Immunoprecipitation (ChIP) Experiments

name of primer	sequence	purpose
hSmad3–1N	5' CTGGAATTCCGCCATGTCGTCCATCCTGCCTTTCACTC 3'	mutagenesis
hSmad3–425C	5' AATGCGGCCGCTAAGACACACTGGAACAGCGGAT 3'	mutagenesis
hSmad3-N218A-S	5' CCAGCACATAATGCCTTGACCTGCAG 3'	mutagenesis
hSmad3-N218A-AS	5' CTGCAGGTCCAAGGCATTATGTGCTGG 3'	mutagenesis
hSmad3-Q222A-S	5' AACTTGGACCTGGCGCCAGTTACCTAC 3'	mutagenesis
hSmad3-Q222A-AS	5' GTAGGTAACCTGGCGCCAGGTGCAAGTT 3'	mutagenesis
hSmad3-P229A-S	5' ACCTACTGCGAGGCGGCCTTCTGGTGC 3'	mutagenesis
hSmad3-P229A-AS	5' GCACCAGAAGGCCGCTCGCAGTAGGT 3'	mutagenesis
PAI-1cDNA sense	5' GTGGTCTGTGTACCGTATC 3'	RT-PCR
PAI-1cDNA antisense	5' GTAGTTGAATCCGAGCTGCC 3'	RT-PCR
GAPDH –F	5' ACCACAGTCCATGCCATCAC 3	RT-PCR
GAPDH-R	5' TCCACCACCCTGTTGCTGTA 3'	RT-PCR
Bio CAGA-4-F	5'–Biotin–CAGACAGTCAGACAGTCAGACAGTCAGACAGT 3'	DNAP
CAGA-4-R	5' ACTGTCTGACTGTCTGACTGTCTGACTGTCTG 3'	DNAP
Bio-PAI-1-F	5'–Biotin–GAGAGTCTGGACACGTGGGGAGTCAGCCG 3'	DNAP
PAI-1-R	5' CGGCTGACTCCCCACGTGTCCAGACTCTC 3'	DNAP
PAI-1chip sense	5' CCTCAACCTCAGCCAGACAAG 3'	ChIP
PAI-1chip antisense	5' CCCAGCCCAACAGCCACAG 3'	ChIP
p21chip sense	5' GAGGTCAGCTGCGTTAGAG 3'	ChIP
p21chip antisense	5' TGCAGAGGATGGATTGTCA 3'	ChIP

amplifications are shown in Table 1. All mutant Smad3 cDNAs were sequenced for verification and found to contain the proper mutation. The recombinant adenoviruses were constructed as described (26). The cDNA of Smad3 (P229A) was cloned into *KpnI* and *NotI* restriction sites of the pAdTrackCMV vector. Plasmid pBS-myc-BirA bearing the myc-tagged bacterial biotin ligase BirA was a generous gift from Dr. John Strouboulis (BRC "A. Fleming", Athens, Greece). The expression vector pCDNA3-Bio has been described previously (27). The mammalian vectors expressing Flag-tagged human wild type SARA and HA-tagged constitutively active ALK5 (CA-ALK5) were generous gifts from Dr. Aris Moustakas (Ludwig Institute for Cancer Research, Uppsala, Sweden).

**Cell Culture and Treatments.** HepG2, HEK293T, HaCaT, MDA-MB-468, and 911 cells were cultured in DMEM, supplemented with 10% FBS and penicillin-streptomycin, in a 37 °C, 5% CO<sub>2</sub> incubator.

**Transient Cell Transfections and Infections with Recombinant Adenoviruses.** Transient transfections in HepG2 and HEK293T cells were performed by the Ca<sub>3</sub>(PO<sub>4</sub>)<sub>2</sub> coprecipitation method using 6 µg of DNA/well when the transfections were performed in six-well plates or 30 µg/plate when transfections were performed in P-100 plates. All adenoviruses were amplified and titrated in 911 cells as described (28). Adenoviral transient infections of HaCaT cells using multiplicity of infection (MOI) = 50 were performed as previously described (29).

**Quantitative Real-Time Reverse Transcription PCR Analysis and Luciferase Assays.** HaCaT cells were infected with adenoviruses expressing GFP or 6myc-tagged Smad3 P229A in the absence or in the presence of an adenovirus expressing the HA-tagged constitutively active form of ALK5, and the cell lysates were processed 24 h later for total RNA extraction using Trizol reagent according to the manufacturer's instructions. The first cDNA strand was synthesized using Superscript reverse transcriptase, and 25 ng of resultant cDNA was used per 25 µL reaction. Each cycle consisted of 30 s at 95 °C, 45 s at 58 °C, and 30 s at 72 °C for a maximum of 35 cycles. Real-time PCR was performed using SYBR GreenER qPCR Supermix on a Stratagene MX3000 and analyzed by using the  $\Delta\Delta C_t$  method. Values were normalized to those obtained for the housekeeping glyceraldehyde 3-phosphate dehydrogenase (GAPDH) gene. The primers used for the amplification of the PAI-1 and GAPDH genes are shown in Table 1. Luciferase assays were performed using the luciferase assay kit from Promega, according to the manufacturer's instructions.

**Indirect Immunofluorescence.** HEK293T and MDA-MB-468 cells were seeded on glass coverslips, 22 × 22 mm, covered with 0.1% gelatin, and incubated for 16–18 h. Cells were transfected with 3 µg of each 6-myc Smad expression vector in the presence or in the absence of a constitutively active TGF $\beta$  type I receptor (3 µg). Cells were washed three times on a slow rotating platform with PBS+/+ (PBS plus 0.9 mM CaCl<sub>2</sub> and 0.5 mM MgCl<sub>2</sub>) and fixed with 3% *p*-formaldehyde in PBS+/+ for 5 min at room temperature. Cells were washed three times with PBS+/+ and permeabilized with 0.5% Triton X-100 in buffer 1 (10× buffer 1: 137 mM NaCl, 5 mM KCl, 1 mM Na<sub>2</sub>HPO<sub>4</sub>, 0.4 mM KH<sub>2</sub>PO<sub>4</sub>, 5.5 mM glucose, 4 mM NaHCO<sub>3</sub>, 2 mM MgCl<sub>2</sub>, 2 mM EDTA, 2 mM EGTA, and 20 mM MES at pH 6.0–6.5) for 5 min at room temperature. Cells were washed three times with PBS+/+ and blocked with PBS+/+/1.5% FBS two times. Cells were incubated with antimyc (9E10), 1:200 dilution or anti-Smad3 (Cell Signaling #9513), 1:50 dilution in

PBS+/+/1.5% FBS for 30 min at 4 °C. Cells were washed three times with PBS+/+/1.5% FBS and incubated with the secondary antibody (goat antimouse Alexa Fluor 488 1:500 dilution in PBS+/+/1.5% FBS) for 30 min at 4 °C in the dark. Cells were washed three times with PBS+/+ in the dark and incubated with DAPI (4 µg/mL) for 5 min. Cells were washed three times with PBS+/+ in the dark and mounted on glass slides using mounting solution (1:1 glycerol/PBS). Cells were observed using a Leica SP fluorescent microscope.

**Western Blot Analysis.** Cell lysates or proteins bound to streptavidin agarose or G-Sepharose beads were subjected to sodium dodecyl sulfate–polyacrylamide gel electrophoresis (SDS–PAGE) and transferred to nitrocellulose membranes (Life Sciences and Schleichers & Schuell), with a Bio-Rad Protean electroblot apparatus. Electrophoresis was performed on 10.5% polyacrylamide gel electrophoresis in 500 mL of 1× TGS (1 L 10× TGS: 30.3 g of Tris, 144.2 g of Glycine, 10 g of SDS at pH 8.3). Nitrocellulose membranes were washed with TBS-T (TBS + 0.05% Tween-20) for 10 min, at room temperature. Nonspecific sites were blocked by soaking the membrane in TBB buffer (1× TBS + 5% nonfat milk and 0.1% Tween-20) for 2 h at 4 °C. Western blotting was performed with a 1:500 dilution of the antimyc and anti-P-Smad3 antibodies or 1:1000 dilution of anti-FLAG M2 and anti-ALK5 antibodies in TBB overnight at 4 °C. The membranes were washed 3 times with TBS-T, for 10 min, at room temperature. As a secondary antibody, we used antimouse or antirabbit horseradish peroxidase-conjugated (HRP) in a 1:10,000 dilution in TBS-T for 1 h at room temperature. In the case of biotinylated proteins, membranes were hybridized directly with HRP-conjugated streptavidin in a 1:20000 dilution for 1 h at room temperature. After 3 washes of 15 min with TBS-T at room temperature, bands were visualized by enhanced chemiluminescent detection on Fuji medical X-ray film (Super RX).

**In Vivo Biotinylation and Protein–Protein Interaction Assay.** The *in vivo* biotinylation assay was performed as described (21, 27). Briefly,  $7.5 \times 10^5$  of HEK293T cells were transfected in 10-cm dishes with 7.5 µg of the pCDNA3-Bio-Smad3 (wt or mutant forms) expression vector in the presence or in the absence of 7.5 µg of pCDNA3-BirA vector expressing the bacterial biotin ligase BirA. For protein–protein interaction assays, HEK293T cells were cotransfected with the above plasmids along with 7.5 µg of expression vectors pCDNA3–6myc-Smad2, pCDNA3–6myc-Smad3 (wt or mutant forms), and pCDNA3–6myc-Smad4, in the presence or in the absence of an expression vector for a constitutively active form of the type I TGF $\beta$  receptor (CA-ALK5, 7.5 µg). Cells were lysed in lysis buffer (20 mM Tris-HCl at pH 7.5, 150 mM NaCl, 10% glycerol, and 1% Triton X-100) and allowed to interact with Streptavidin agarose beads for 3 h at 4 °C in a rotating platform. Beads were washed three times with lysis buffer and centrifuged at 4,000 rpm for 1 min at room temperature. Bound proteins as well as the starting material (input) were subjected to SDS–PAGE followed by immunoblotting as described above.

**Coimmunoprecipitations Assays.** Transfected HEK293T cells were washed with ice-cold PBS and collected in PBS. Cells were pelleted by centrifugation at 5000 rpm for 5 min at 4 °C and resuspended in lysis buffer (20 mM Tris/HCl, pH 7.5, 150 mM NaCl, 10% glycerol, and 1% Triton X-100) supplemented with protease inhibitors. Lysates were rotated on a platform for 30 min at 4 °C. Extracts were collected by centrifugation at 13000 rpm for 5 min at 4 °C, then precleared by incubation with 35 µL of Protein G–Sepharose Fast Flow beads pre-equilibrated with



lysis buffer. Supernatants were incubated with a proper dilution of the first antibody (anti-flag or anti-GST) on a rotating platform overnight at 4 °C, followed by incubation with 35  $\mu$ L of Protein G–Sephacrose Fast Flow beads for 3 h. Beads were washed three times in lysis buffer, precipitated, and resuspended in 4 $\times$  SDS loading buffer.

**Chromatin Immunoprecipitation (ChIP) Assay.** HEK293T cells grown in P-100 plates were transfected with expression vectors for wild type flag-Smad3 (7.5  $\mu$ g) or flag-Smad3P229A (7.5  $\mu$ g), and the constitutively active form of the type I TGF $\beta$  receptor (ALK5-ca, 5  $\mu$ g) along with the hPAI-1 (–800/+71)-Luc (2  $\mu$ g). The ChIP assay was performed as described previously (30) using an anti-flag antibody. Immunoprecipitated chromatin was analyzed by PCR using primers corresponding to the –795/–615 region of the human plasminogen activator inhibitor-1 (PAI-1) promoter and to the –1416/–1263 region of the human cell cycle inhibitor p21<sup>CDKN1A</sup> promoter. The sequence of the primers is given in Table 1. The products of the PCR amplifications were analyzed by agarose gel electrophoresis.

**DNA Affinity Precipitation (DNAP) Assays.** Transfected HEK293T cells were washed with ice-cold PBS, collected by centrifugation at 5000 rpm at 4 °C for 5 min and resuspended in lysis buffer (20 mM Tris-HCl at pH 7.5, 150 mM NaCl, 10% glycerol, and 1% Triton X-100) supplemented with protease inhibitors. Lysates were rotated on a rotating platform for 30 min at 4 °C and purified by centrifugation at 13000 rpm for 5 min at 4 °C. Dynabeads were washed once with 1 $\times$  B&W buffer [5 mM Tris/HCl (pH 7.5), 0.5 mM EDTA, and 1 mM NaCl], mixed with 0.58  $\mu$ M of biotinylated PCR fragment corresponding to a biotinylated oligonucleotide containing four copies of a canonical Smad binding element (4 $\times$  SBE) or a biotinylated double stranded oligonucleotide corresponding to the –688/–660 region of the plasminogen activator inhibitor 1 gene and incubated at room temperature for 15 min. The beads were washed twice with 1 $\times$  B&W buffer and once with 1 $\times$  BBRC buffer (10% glycerol, 10 mM Tris/HCl at pH 7.5, 50 mM KCl, 4 mM MgCl<sub>2</sub>, and 0.2 mM EDTA). The cell extracts were incubated overnight at 4 °C with the pre-equilibrated streptavidin Dynabeads in 1 $\times$  BBRC buffer. Each reaction mixture included 100–150  $\mu$ g of total cell extracts, 8  $\mu$ g of competitor poly (dI/dC) and the DNA-coupled Dynabeads in a total reaction volume of 300  $\mu$ L. 6myc-Smad3

(wt or mutant forms) bound to the oligonucleotides was detected by SDS–PAGE and immunoblotting using the mouse monoclonal anti-c-myc 9E10 antibody

## RESULTS

**Glutamine 222 Plays an Important Role in Smad3 Homo- and Hetero-Oligomerization in Response to TGF $\beta$  Stimulation.** We have shown previously that an internal deletion in the linker region of Smad3 (Smad3  $\Delta$ 200–230) compromised TGF $\beta$  signaling by affecting the nuclear functions of Smad3 such as the interaction with the histone acetyltransferase p/CAF and the transcriptional activation of TGF $\beta$  target promoters (21). Amino acid residues 200–230 in Smad3 are located within a nonconserved region at the C-terminal end of the linker (Figure 1). A closer inspection of this region revealed that out of these 30 amino acids, only three are well conserved among all TGF $\beta$ - and BMP-regulated Smads and Smad4. These amino acids are two prolines at positions 209 and 229 (P209, P229) and a glutamine at position 222 (Q222). Proline 209 is part of a Ser/Pro motif which was shown previously to serve as a target for mitogen-activated protein kinases such as ERK (31). Mutagenesis of serine 208 to alanine decreased ERK phosphorylation and increased the ability of Smad3 to stimulate a Smad target gene, suggesting that ERK phosphorylation inhibits Smad3 activity (31). In BMP-regulated Smads only, this proline residue is located in the vicinity of a PPXY motif (residues 224–227 in Smad1, Figure 1) which is recognized by the ubiquitin ligase Smurf1 (32). In an attempt to identify novel residues in this part of the linker that may play important roles in Smad3 regulation, we focused our attention to conserved residues Q222 and P229 as well as to an amino acid residue, asparagine 218 (N218), that is not conserved among the different Smads. As shown in Figure 1, this position is occupied by an arginine in Smad1 (R257), a glutamate in Smad4 (E307), and a serine in Smad2 (S260) and Smad5 (S257).

We generated Smad3 mutants bearing individual substitutions of these amino acids to alanine (Smad3 N218A, Q222A, and P229A), and we monitored their functional properties along the TGF $\beta$  signaling pathway. First, we looked at their phosphorylation in response to TGF $\beta$  stimulation. To achieve this goal, we took advantage of an *in vivo* Smad biotinylation assay that we established recently, which is based on the fusion of Smads with

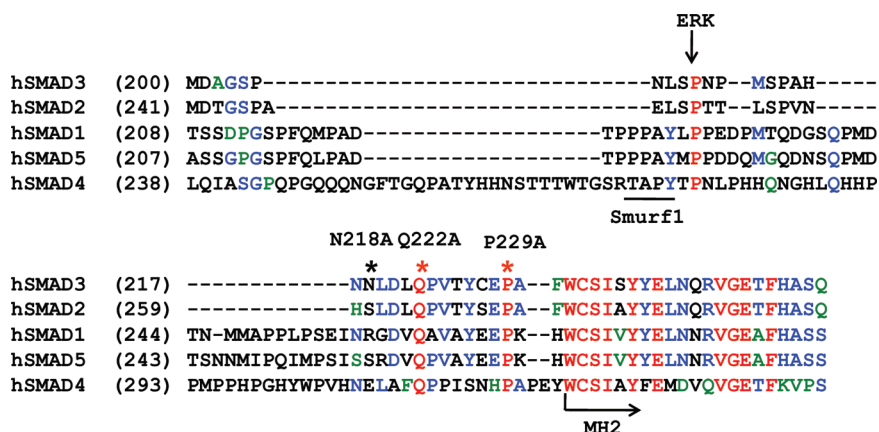
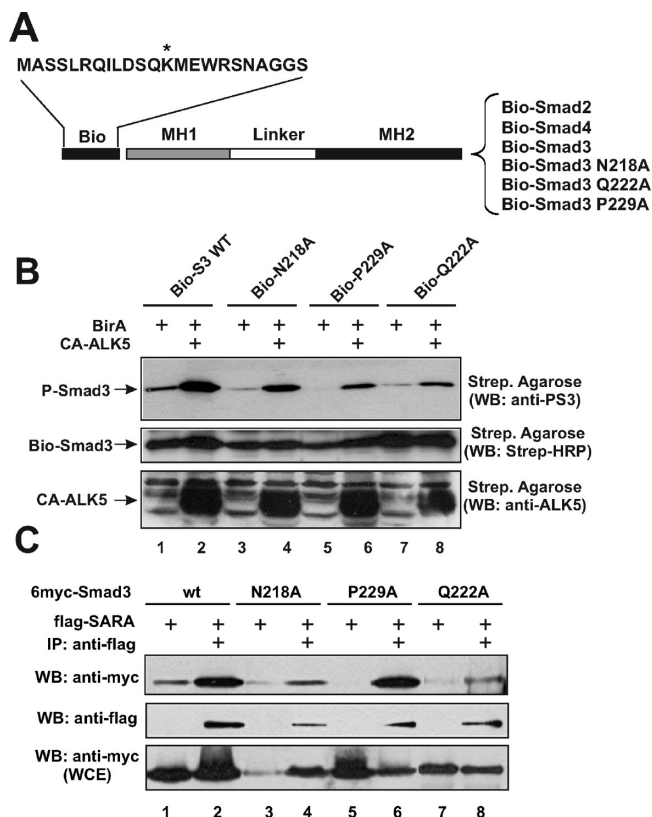


FIGURE 1: Amino acid sequence homology in the linker regions of R-Smads and Smad4. Amino acid sequence homology between TGF $\beta$  and BMP-regulated Smads as well as Smad4, in the 200–230 region of Smad3, containing the amino acid residues N218, Q222, and P229 that were mutagenized in the present study. The amino acid substitutions that were introduced to Smad3 are shown by asterisks. A Ser/Pro motif in Smad3 that serves as target for ERK MAP kinase and a recognition motif for the ubiquitin ligase Smurf1 are also shown. Totally conserved amino acids are shown in red. Amino acids with lower degree of homology among Smads are shown in blue and green.



**FIGURE 2:** Conserved residue glutamine 222 in the Smad3 linker is required for interaction with the cytoplasmic adaptor SARA. (A) Schematic representation of wild type Smad2, Smad3, Smad4, and Smad3 mutants N218A, Q222A, and P229A tagged with the Bio peptide at their N-terminus. The amino acid sequence of the Bio peptide that serves as a recognition site for the bacterial biotin ligase BirA is shown. The lysine residue that is biotinylated by BirA is indicated with an asterisk. (B) HEK293T cells were transfected with vectors expressing wild type Bio-Smad3 or Bio-Smad3 mutants N218A, Q222A, and P229A, and BirA in the absence or in the presence of an expression vector for the constitutively active ALK5 receptor (CA-ALK5). The biotinylated proteins were purified by streptavidin affinity chromatography, and the phosphorylation status of the purified proteins was examined by Western blot using an antibody against phosphorylated Smad3 (anti-PS3). Smad biotinylation was monitored by Western blotting using HRP-conjugated streptavidin (Strep-HRP). CA-ALK5 expression was monitored by Western blotting using an antibody against ALK5. (C) HEK293T cells were transfected with expression vectors for wild type flag-tagged SARA and 6myc-Smad3 or 6myc-Smad3 mutants N218A, Q222A, and P229A, and subjected to immunoprecipitation (IP) using a mouse monoclonal anti-flag antibody or a nonspecific (anti-GST) antibody as a control. The immunoprecipitated proteins as well as the starting material (WCE, whole-cell extract) were analyzed by SDS/PAGE and Western blotting (WB) using the monoclonal anti-myc antibody. Immunoblots were stripped and reprobed with anti-flag antibody to detect the immunoprecipitated flag-tagged SARA.

the Bio peptide bearing the recognition sequence of the bacterial ligase BirA (Figure 2A) (33). This facilitates the purification of the *in vivo* biotinylated protein via streptavidin affinity chromatography. We used the Bio-Smad3 plasmids along with an expression vector for BirA to transfect HEK293T cells in the absence or in the presence of the constitutively active type I TGF $\beta$  receptor (CA-ALK5) used here to mimic the TGF $\beta$  stimulation (34). The phosphorylation status of the purified proteins was examined by immunoblotting using an antibody raised against Smad3 phosphorylated at its C-terminal SSXS motif. As shown in Figure 2B, none of the Smad3 mutants lost its ability to be phosphorylated by the constitutively active ALK5 receptor.

We then analyzed the physical interaction of the three Smad3 mutants with the endosomal protein SARA. SARA is a FYVE domain protein that interacts directly with Smad2 and Smad3, and recruits them to the TGF $\beta$  receptor type I for phosphorylation (35). Phosphorylation of R-Smads induces their dissociation from SARA with concomitant formation of R-Smad/Smad4 complexes and their nuclear translocation (35). The interaction of wild type or mutant Smad3 proteins with SARA was performed by coimmunoprecipitation experiments as described in Materials and Methods. As shown in Figure 2C, wild type 6myc-Smad3 interacted efficiently with flag-tagged SARA in agreement with previous findings (36). The 6myc-Smad3 N218A and P229A mutants interacted with SARA as efficiently as wild type Smad3 (note the lower levels of expression of 6myc-Smad3 N218A mutant in this experiment) (lanes 4 and 6). In contrast, 6myc-Smad3 Q222A mutant showed a weak but detectable interaction with flag-SARA (lane 8).

The formation of Smad oligomers in response to TGF $\beta$  stimulation is at the heart of TGF $\beta$  signaling in mammalian cells and disruption of Smad oligomerization is frequently observed in cancer patients (10, 37). We thus sought to investigate the oligomerization properties of the Smad3 linker mutants that we generated. Using the *in vivo* biotinylation system described above, we first analyzed the ability of the wild type and mutant Smad3 proteins to form oligomers with other Smads (i.e., hetero-oligomerization). As shown in Figure 3A, wild type 6myc-Smad3 and the 6myc-Smad3 N218A and P229A mutants interacted efficiently with biotinylated Smad2 (Bio-Smad2) in the presence of BirA ligase (lanes 2, 8, and 11, respectively) and this interaction was greatly enhanced in the presence of the constitutively active ALK5 receptor (CA-ALK5) (lanes 3, 9, and 12, respectively). In contrast, no interaction between Bio-Smad2 and the 6myc-Smad3 Q222A mutant could be observed either in the absence (lane 5) or in the presence (lane 6) of CA-ALK5. The top and bottom panels of Figure 3A show the detection of 6myc-Smad3 proteins on the streptavidin agarose beads and the whole cell extracts, respectively, by immunoblotting using the anti-myc antibody, whereas the middle panels show the detection of biotinylated Smad2 protein on the streptavidin agarose beads by blotting using HRP-conjugated streptavidin. Identical results were obtained when the wild type and mutant 6myc-Smad3 proteins were tested for interaction with biotinylated Smad4 (Figure 3B).

In summary, the data of Figure 3A and B revealed that the replacement of the conserved polar amino acid glutamine at position 222 in the linker region of Smad3 protein with the nonpolar amino acid alanine abolished the hetero-oligomerization properties of this protein. This did not happen when the nonpolar amino acid proline at position 229 or the polar but nonconserved amino acid asparagine at position N218 was replaced by alanine.

We then investigated the homo-oligomerization properties of the Smad3 mutants using the same protein-protein interaction system. As shown in Figure 3C, 6myc-Smad3 N218A and P229A mutants, similar to wild type 6myc-Smad3, retained their ability to form homo-oligomers in the presence of CA-ALK5 (lanes 3, 9, and 12). In contrast, 6myc-Smad3 Q222A mutant had lost its ability to form homo-oligomers in the presence of CA-ALK5 (lane 6).

In conclusion, the findings of Figure 3 indicated that glutamine 222 in the linker region of Smad3 is required for Smad3 homo- and hetero-oligomerization in response to TGF $\beta$  stimulation.

**Effect of the Q222A Mutation on the Nuclear Translocation of Smad3 in Response to TGF $\beta$  Stimulation.** Next, we

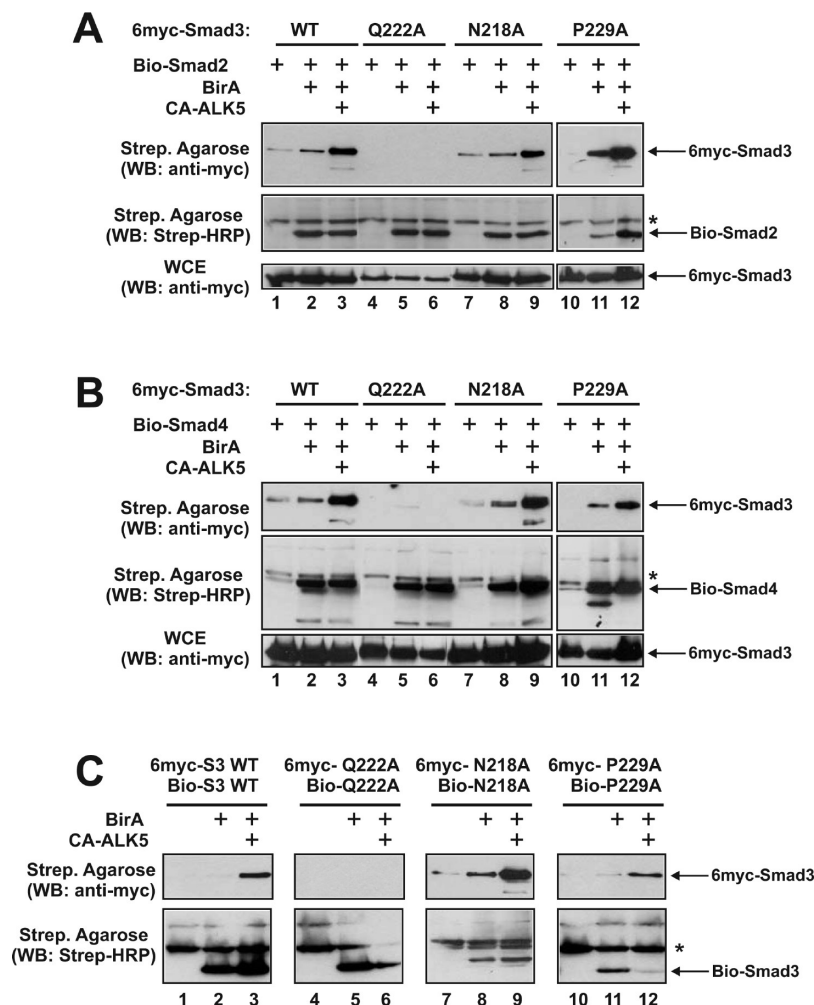


**FIGURE 3:** Glutamine 222 plays an important role in Smad3 homo- and hetero-oligomerization in response to TGF $\beta$  stimulation. (A,B) Hetero-oligomerization assays. HEK293T cells were transfected with different combinations of expression vectors for Bio-Smad2, Bio-Smad4, and Bio-Smad3 along with wild type 6myc-Smad3 or 6myc-Smad3 mutants N218A, Q222A, and P229A, and BirA and CA-ALK5 as indicated on top. The concentrations of plasmids used and the protocol of the protein–protein interaction assay are described in detail in Materials and Methods. Immunoblottings were performed using the antimyc monoclonal antibody for the detection of myc-tagged Smad3 and HRP-conjugated streptavidin for the detection of biotinylated Smad2 and Smad4 proteins. (C) Homo-oligomerization assays. HEK293T cells were transfected with vectors expressing wild type Bio-Smad3, Bio-Smad3 N218A, Bio-Smad3 Q222A, or Bio-Smad3 P229A along with their 6-myc tagged counterparts and BirA in the absence or in the presence of expression vector for the constitutively active ALK5 receptor (CA-ALK5). The biotinylated proteins were purified by streptavidin affinity chromatography. Immunoblottings were performed using the antimyc monoclonal antibody for the detection of myc-tagged Smad3 proteins. In all panels, nonspecific proteins detected by streptavidin-HRP are shown with asterisks.

examined the ability of the Smad3 linker mutants to translocate to the nucleus in response to TGF $\beta$  stimulation. For this purpose, HEK293T fibroblasts were transiently transfected with expression vectors for 6myc-Smad3 (wild type or mutant) and Bio-Smad4 in the presence or in the absence of an expression vector for the constitutively active TGF $\beta$  type I receptor (CA-ALK5). The subcellular localization of 6myc-Smad3 proteins was monitored by indirect immunofluorescence using an antimyc antibody followed by a secondary Alexa Fluor antibody. Nuclei were stained with DAPI. As shown in Figure 4, all four 6myc-Smad3 proteins showed a predominant cytoplasmic staining in the absence of CA-ALK5 in HEK293T cells. In the presence of CA-ALK5, staining of wt 6myc-Smad3, 6myc-Smad3 N218A, and 6myc-Smad3 P229A was predominantly nuclear, whereas no nuclear staining was observed in the case of 6myc-Smad3 Q222A. These findings showed that mutation Q222A compromised the translocation of activated Smad3 to the nucleus.

To investigate the requirement of Smad4 for the nuclear translocation of activated Smad3 mutants, we repeated the

immunofluorescence experiment of Figure 4 in MDA-MB-468 cells that lack endogenous Smad4 expression (38). As shown in Figure 5, wild type Smad3 and all three Smad3 mutants were localized in the cytoplasm of MDA-MB-468 cells in the absence of CA-ALK5. In the presence of CA-ALK5, partial or complete nuclear staining was observed in the case of wild type N218A and P229A Smad3 proteins suggesting that activated Smad3 proteins can translocate to the nucleus as homo-oligomers (in the absence of Smad4) albeit to a lower degree. However, no nuclear staining was observed in the case of the Smad3 Q222A mutant. These data, combined with the data of Figure 3 showing that the Smad3 Q222A mutant is unable to form both hetero- and homo-oligomers, indicated that Smad3 proteins cannot translocate to the nucleus as monomers.

*Conserved Amino Acid Residues Q222 and P229 in the Linker Region of Smad3 Are Required for Smad-Mediated Transactivation.* Transactivation experiments in human hepatoblastoma HepG2 cells showed that wild type Smad3 strongly transactivated (37-fold) a Smad-responsive promoter



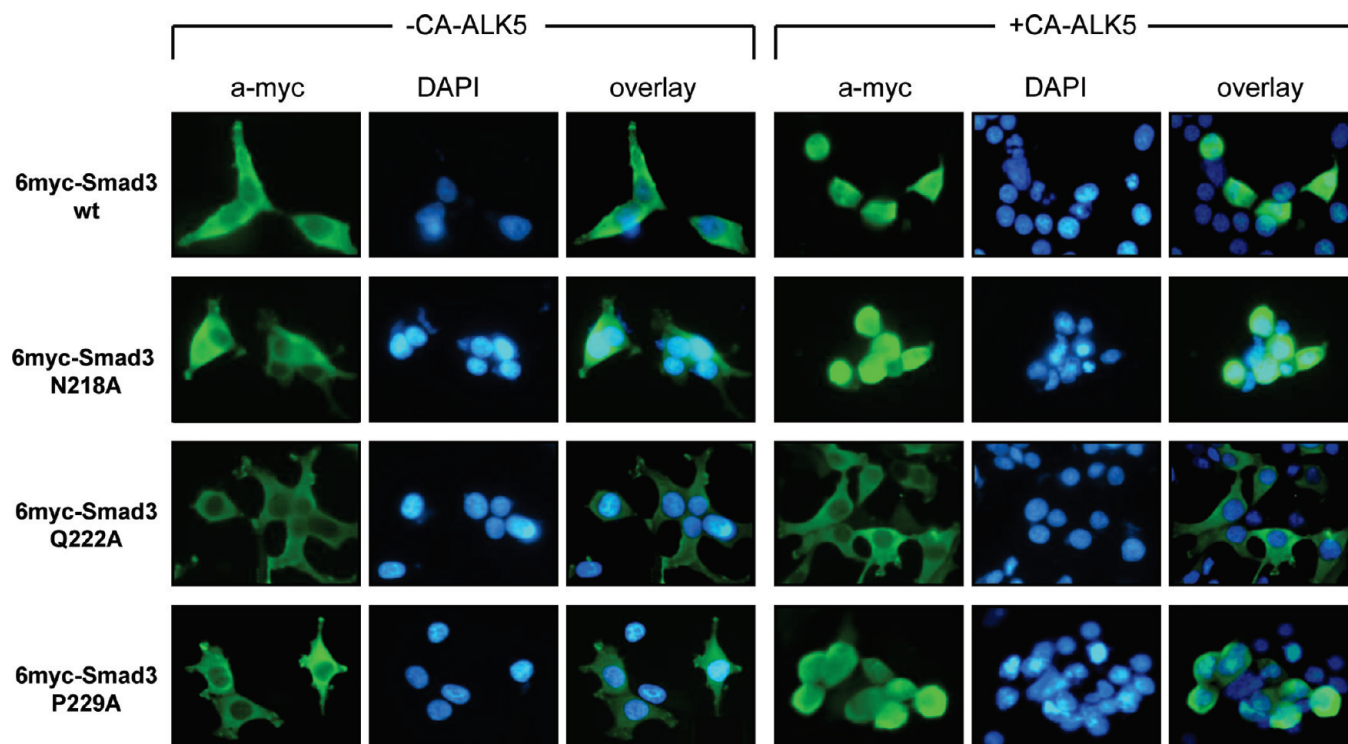


FIGURE 4: Mutation Q222A inhibited the nuclear translocation of Smad3 in response to TGF $\beta$  stimulation. HEK293T were transfected with expression vectors for wild type 6myc-Smad3 or 6myc-Smad3 mutants N218A, Q222A, and P229A in the absence (–CA-ALK5) or in the presence (+CA-ALK5) of the constitutively active ALK5 receptor and Bio-Smad4. Immunofluorescence experiment was performed using the antimyc monoclonal antibody followed by a secondary antimouse Alexa Fluor antibody. Nuclei were stained with DAPI.

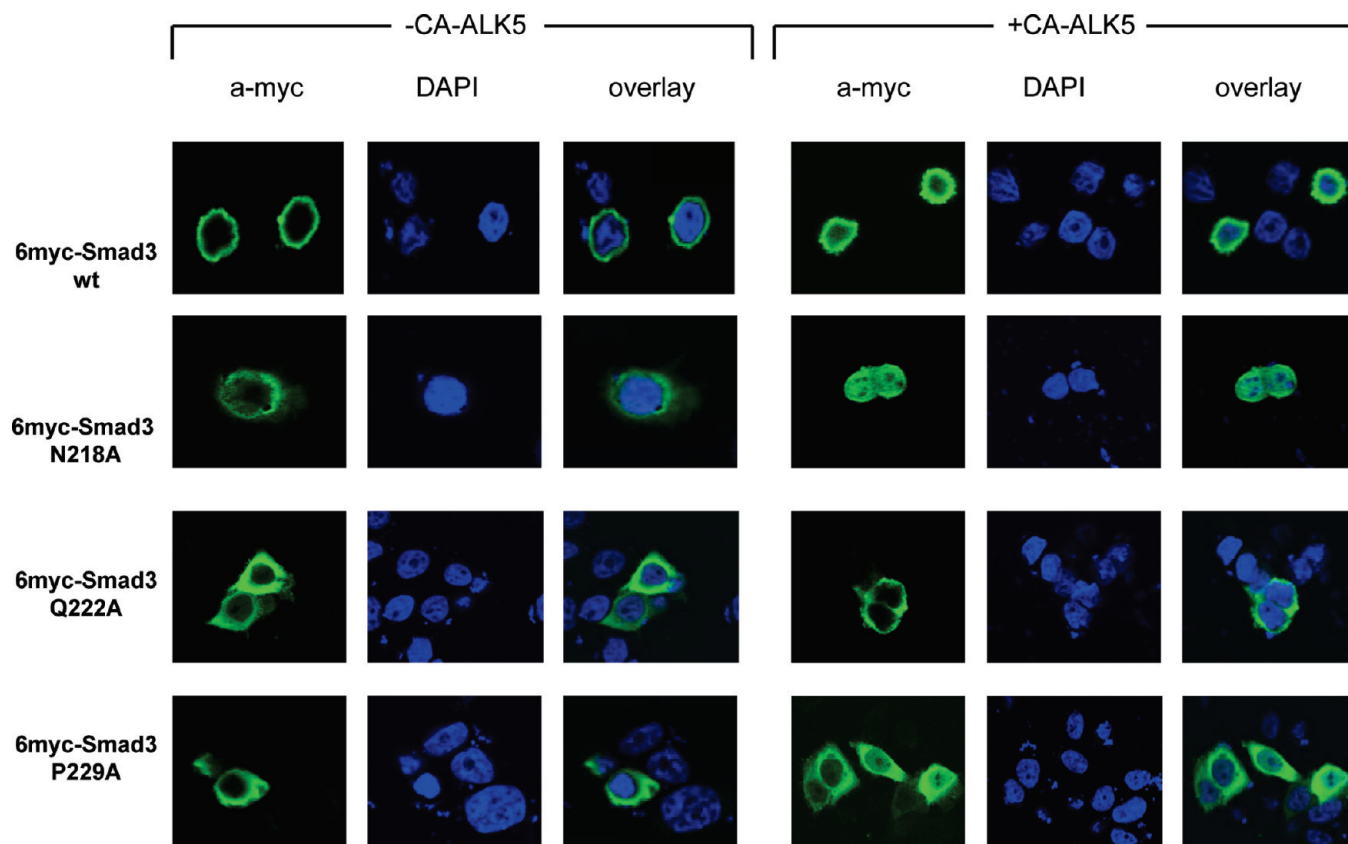


FIGURE 5: Smad homo- and/or hetero-oligomerization is required for TGF $\beta$ -induced nuclear translocation. MDA-MB-468 cells were transfected with expression vectors for wild type 6myc-Smad3 or 6myc-Smad3 mutants N218A, Q222A, and P229A in the absence (–CA-ALK5) or in the presence (+CA-ALK5) of the constitutively active ALK5 receptor. Immunofluorescence experiment was performed using the antimyc monoclonal antibody followed by a secondary antimouse Alexa Fluor antibody. Nuclei were stained with DAPI.

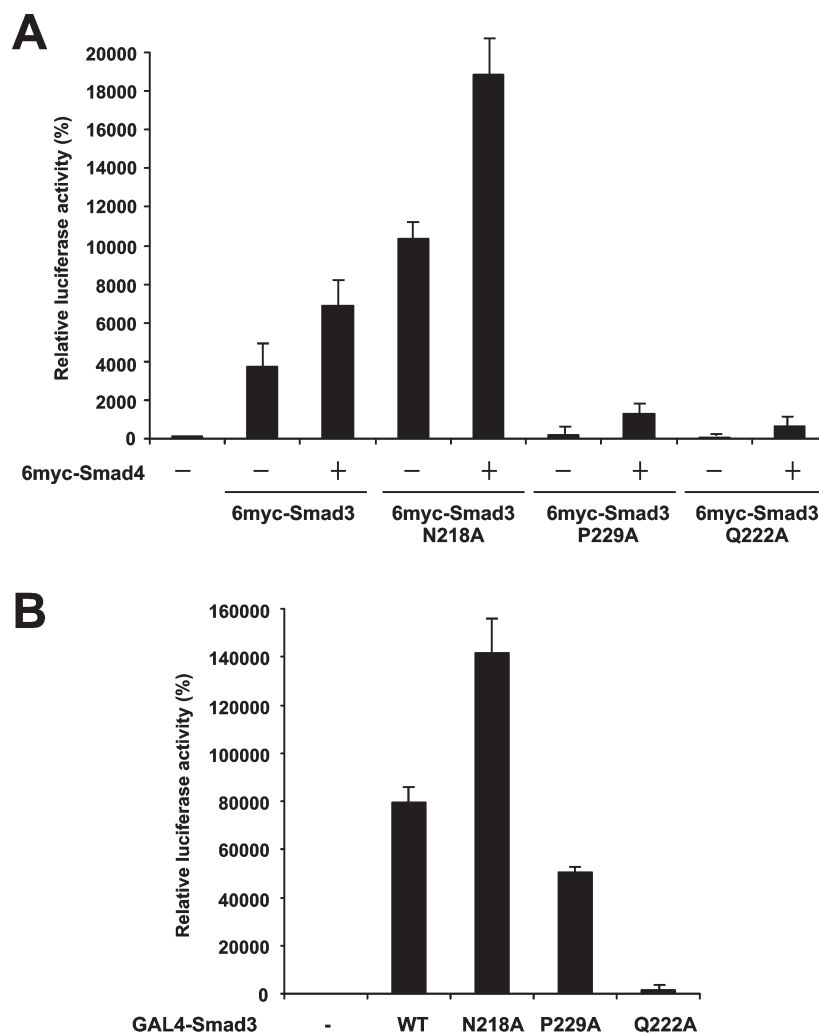


FIGURE 6: Conserved amino acid residues Q222 and P229 in the linker region of Smad3 are required for Smad-mediated transactivation. (A) HepG2 cells were transfected with expression vectors for wild type 6myc-Smad3 (1  $\mu$ g) or 6myc-Smad3 mutants N218A, Q222A, and P229A (1  $\mu$ g) in the absence or presence of expression vector for 6myc-Smad4 (1  $\mu$ g) along with the p(CAGA)<sub>12</sub>-E1B-Luc (1  $\mu$ g). (B) HepG2 cells were transfected with the indicated GAL4-Smad3 fusion protein along with the pG5-E1B-Luc reporter plasmid. In both panels, the CMV- $\beta$ -gal plasmid expressing  $\beta$ -galactosidase (1  $\mu$ g) was included in each sample for normalization of transfection variability. Luciferase activity was determined in cell lysates at 48 h after transfection, and the relative values ( $\pm$  S.E.M.) from at least three independent experiments performed in duplicate are shown in the histogram.

containing 12 tandem copies of a Smad binding element derived from the plasminogen activator inhibitor-1 (PAI-1) gene (CAGA<sub>12</sub>) and that this activation was enhanced further by the simultaneous expression of Smad4 (68-fold) (Figure 6A). Interestingly, 6myc-Smad3 N218A showed an enhanced transactivation potential compared with that of wild type 6myc-Smad3 either in the absence or in the presence of Smad4 (104-fold and 190-fold transactivation, respectively). In sharp contrast, overexpression of either 6myc-Smad3 P229A or 6myc-Smad3 Q222A failed to transactivate the CAGA<sub>12</sub> promoter in the absence of 6myc-Smad4, whereas in the presence of 6myc-Smad4, the transactivation of the CAGA<sub>12</sub> promoter was reduced by 90% and 96%, respectively, relative to the transactivation by wild type 6myc-Smad3 (Figure 6A). These findings were a first indication that specific conserved residues in the linker region of Smad3 may be essential for the nuclear functions of this protein in mammalian cells such as DNA binding and transcriptional activation.

In the transactivation experiment of Figure 6A in which the CAGA<sub>12</sub> reporter was used, the transcriptional read-out depends

on the direct binding of Smads to the numerous Smad binding elements that are present in this artificial promoter. Thus, the deficiency in the transactivation potential that was observed in the case of the Smad3 P229A and Q222A mutants (Figure 6A) could be accounted for by defects in the DNA binding properties of both mutants. If this is indeed the case, then these mutants should exhibit normal (similar to wild type) transactivation properties when fused with a heterologous DNA binding domain. To address this possibility, we took advantage of the GAL4 transactivation system. For this purpose, we fused the three Smad3 linker mutants with the DNA binding domain of the yeast transactivator GAL4 and examined their ability to transactivate an artificial promoter (G<sub>5</sub>B) consisting of 5 tandem GAL4 DNA binding sites placed in front of the firefly luciferase gene. As shown in Figure 6B, GAL4-Smad3 (wild type) strongly transactivated the G<sub>5</sub>B promoter (800-fold). In agreement with the findings of Figure 6A, the GAL4-Smad3 N218A mutant had a higher transactivation capacity than that of wild type Smad3 (1400-fold transactivation of the G<sub>5</sub>B promoter), whereas the GAL4-Smad3 Q222A mutant was transcriptionally silent. The total lack of transactivation by the GAL4-Smad3 Q222A mutant



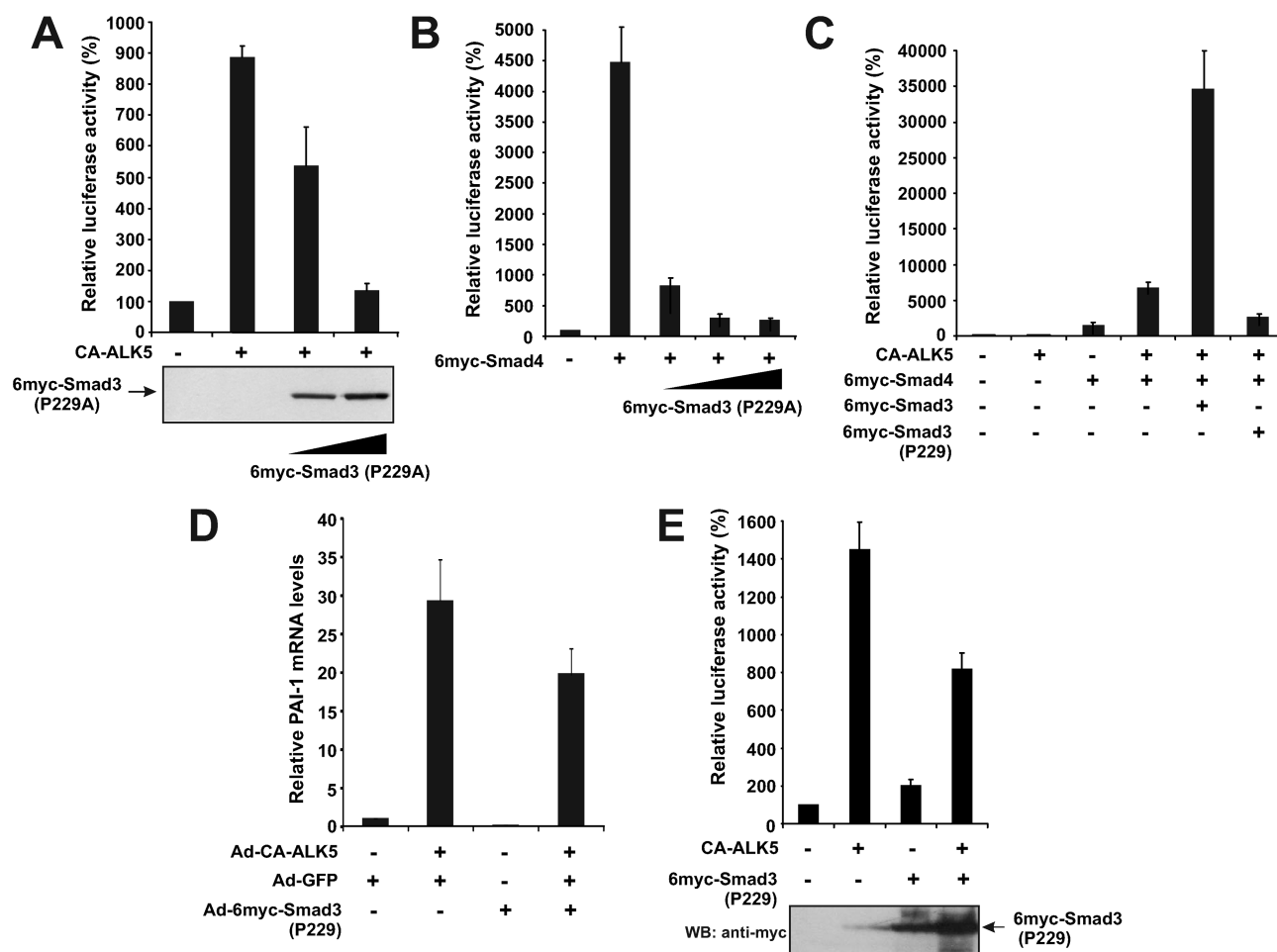


**FIGURE 7:** Smad3 P229A inhibits the transcriptional activation of TGF $\beta$  target genes. (A) HepG2 cells were transfected with the p(CAGA)<sub>12</sub>-E1B-Luc (1  $\mu$ g) reporter plasmid in the absence or in the presence of an expression vector for the constitutively active ALK5 receptor (CA-ALK5) and increasing concentrations of an expression vector for 6myc-Smad3 P229A. An immunoblot showing the levels of expression of the 6myc-Smad3 P229A mutant in the transfected cells is shown below the graph. (B) HepG2 cells were transfected with the p(CAGA)<sub>12</sub>-E1B-Luc reporter plasmid (1  $\mu$ g) in the absence or in the presence of an expression vector for 6myc-Smad4 and increasing concentrations of an expression vector for 6myc-Smad3 P229A. (C) MDA-MB-468 cells were transfected with the reporter vector p(CAGA)<sub>12</sub>-E1B-Luc (1  $\mu$ g) along with different combinations of expression vectors for the constitutively active ALK5 receptor (CA-ALK5), 6myc-Smad4, 6myc-Smad3, and 6myc-Smad3 P229A. (D) HaCaT cells were infected with a control adenovirus (ad-GFP) or with a recombinant adenovirus expressing Smad3 P229A (ad-Smad3 P229) in the absence (–) or in the presence of an adenovirus expressing the constitutively active ALK5 receptor (ad-CA-ALK5) as indicated. Quantitative real-time PCR analysis was performed as described in Materials and Methods using primers specific for the PAI-1 gene and for the housekeeping GAPDH gene which was used for normalization. (E) HepG2 cells were transfected with the (–700) PAI-1-Luc (1  $\mu$ g) reporter plasmid in the absence or in the presence of an expression vector for the constitutively active ALK5 receptor (CA-ALK5) and an expression vector for 6myc-Smad3 P229A. An immunoblot showing the levels of expression of the 6myc-Smad3 P229A mutant in the transfected cells is shown below the graph. In panels A–C and E, the CMV- $\beta$ -gal plasmid expressing  $\beta$ -galactosidase (1  $\mu$ g) was included in each sample for normalization of transfection variability. Luciferase activity was determined in cell lysates at 48 h after transfection, and the relative values ( $\pm$  S.E.M.) from at least three independent experiments performed in duplicate are shown in the histograms.

was not due to a defect in nuclear accumulation of this hybrid protein as demonstrated by immunofluorescence (Supporting Information, Figure 1). Interestingly however, in the GAL4 system, Smad3 P229 was not silent but displayed a transcriptional activity that was 40% lower than the activity of wild type Smad3 (500-fold activation of the G<sub>3</sub>B promoter). This finding strongly suggested that the failure of this mutant to transactivate Smad-responsive promoters (Figure 6A) could be accounted for by a defect in DNA binding (see below).

**Smad3 P229A Inhibits TGF $\beta$  Signaling.** The profile of the Smad3 P229A mutant, i.e., normal TGF $\beta$ -induced phosphorylation, oligomerization, and nuclear translocation but defective transactivation, prompted us to investigate whether this mutated Smad3 protein has dominant negative properties. As shown in Figure 7A, overexpression of CA-ALK5 in HepG2 cells activated the CAGA<sub>12</sub> promoter, but this activation was strongly inhibited

by the coexpression of 6myc-Smad3 P229 in a dose-dependent fashion. Similarly, 6myc-Smad3 P229A inhibited the transactivation of the CAGA<sub>12</sub> promoter by overexpressed 6myc-Smad4 in a dose dependent manner in HepG2 cells (Figure 7B). The dominant negative effect of Smad3 P229A on Smad4 was also examined in breast cancer cell line MDA-MB-468 that does not express endogenous Smad4 (38). As shown in Figure 7C, CA-ALK5 could not transactivate the CAGA<sub>12</sub> promoter in these cells because of the absence of endogenous Smad4, whereas overexpression of wild type 6myc-Smad4 restored the response of this promoter to CA-ALK5. Wild type 6myc-Smad3 enhanced the CA-ALK5 and 6myc-Smad4 mediated transactivation of the CAGA<sub>12</sub> promoter approximately 5-fold. In contrast, 6myc-Smad3 P229A inhibited the transactivation of the CAGA<sub>12</sub> promoter by CA-ALK5 and 6myc-Smad4 by 60% (Figure 7C).

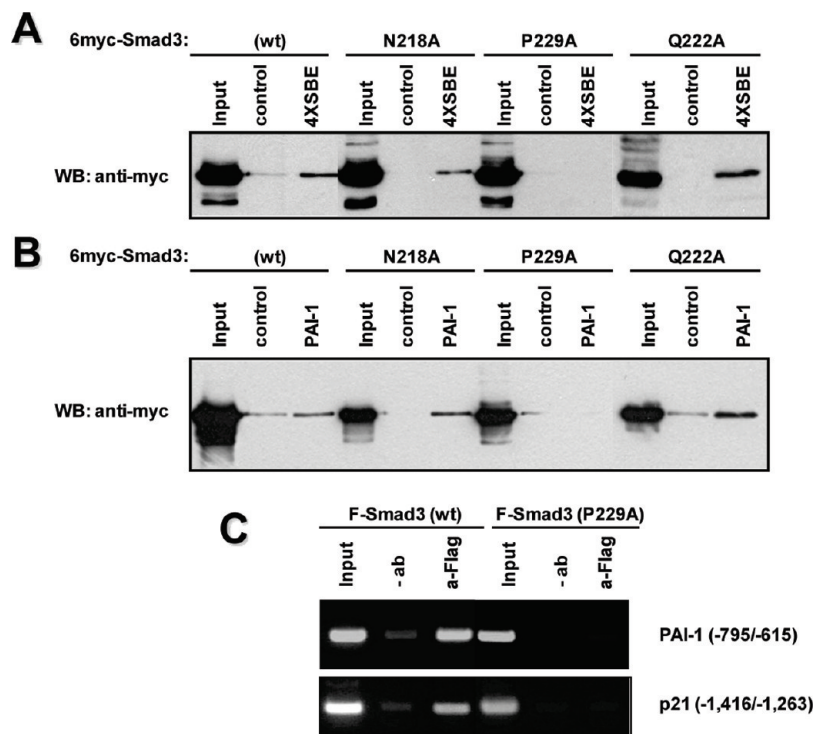


FIGURE 8: Mutation P229A in the Smad3 linker abolished DNA binding *in vitro* and *in vivo*. (A,B) DNA affinity precipitation experiment using extracts from HEK293T cells that had been transfected with an expression vector for wild type 6myc-Smad3 or 6myc-Smad3 mutants N218A, Q222A, and P229A. Biotinylated double stranded oligonucleotides bearing 4 copies of a consensus Smad binding element (4XSBE) (A) or the  $-688/-660$  region of the human plasminogen activator inhibitor  $-1$  gene (PAI-1) (B) were coupled to streptavidin agarose beads and incubated with the cell lysates as described in Materials and Methods. Bound proteins were analyzed by SDS-PAGE and immunoblotting using an antibody against the 6myc epitope tag of Smad3 proteins. (C) Chromatin immunoprecipitation in HEK293T cells ectopically expressing flag-Smad3 (wt) or flag-Smad3 (P229A) as described in Materials and Methods. Immunoprecipitations were performed using the anti-flag antibody or no antibody as a control ( $-ab$ ). PCR was performed using primers corresponding to the  $-795/-615$  region of the human PAI-1 promoter or the  $-1,416/-1,263$  region of the human p21<sup>CDKN1A</sup> gene.

To confirm that the dominant negative effect of Smad3 P229A on TGF $\beta$  signaling can also be exerted on the expression of endogenous TGF $\beta$  target genes, HaCaT cells were infected with recombinant adenoviruses expressing CA-ALK5 (Ad-CA-ALK5), 6myc-Smad3 P229A (Ad-6myc-Smad3 P229A), or GFP (Ad-GFP) as a control. The mRNA levels of the endogenous PAI-1 gene or of the GAPDH gene (normalization standard) were measured by quantitative real-time PCR. As shown in Figure 7D, Ad-6myc-Smad3 P229A, but not Ad-GFP, inhibited the Ad-CA-ALK5-induced transcription of the PAI-1 gene in HaCaT cells. In agreement with this finding, 6myc-Smad3 P229A inhibited the CA-ALK5-induced transactivation of the PAI-1 promoter in HepG2 cells (Figure 7E). Thus, the combined data of Figure 7 showed that the Smad3 P229A mutant inhibits TGF $\beta$  signaling when overexpressed in mammalian cells.

*Proline 229 in the Linker Region of Smad3 Is Essential for DNA Binding in Vitro and in Vivo.* We finally sought to examine the possibility that the three mutations in the linker region of Smad3 have affected its DNA binding properties. To address this, we first performed DNA affinity precipitation assays (DNAP) *in vitro* using 6myc-Smad3 proteins overexpressed in HEK293T cells as described in Materials and Methods. As shown in Figure 8A, wild type 6myc-Smad3 and the 6myc-Smad3 mutants N218 and Q222A interacted with a biotinylated oligonucleotide bearing four copies of the consensus Smad binding element 5' CAGAC 3' (4 $\times$  SBE) (34). In contrast, the 6myc-Smad3 P229A mutant could not bind to the SBE, suggesting that the P229A mutation has affected the DNA binding properties of Smad3. Similar results were obtained when

a probe derived from the promoter of the plasminogen activator inhibitor 1 (PAI-1) gene (region  $-688/-660$ ) was utilized (Figure 8B) (39).

To prove that the P229A linker mutation affected the DNA binding properties of Smad3, we performed *in vivo* chromatin immunoprecipitation assays in HEK293T cells expressing flag-Smad3 (wt) or flag-Smad3 (P229A) along with CA-ALK5 to ensure the nuclear accumulation of the exogenous proteins (Figure 4). As shown in Figure 8C, wild type flag-Smad3 (F-Smad3) was recruited to the PAI-1 ( $-795/-615$ ) and p21 ( $-1,416/-1,263$ ) promoter regions (lane 3), whereas no recruitment of the flag-Smad3 P229A mutant to these promoters could be detected (lane 6).

## DISCUSSION

*Regulation of Smad Function by the Linker Region.* Smad proteins are key effectors of TGF $\beta$  signaling in mammalian cells and other species (6, 7). The multiple functions of Smads include phosphorylation and oligomerization in response to TGF $\beta$  stimulation, translocation to the nucleus, sequence-specific DNA binding, and interaction with coregulatory molecules such as coactivators or corepressors (6, 7). All of these activities are clustered in two separate domains called the MH1 and MH2 at the N-terminal and the C-terminal ends of the proteins, respectively (6, 7). The region that connects the MH1 and MH2 domains is called the linker, and it is generally believed that it has no specific functions other than allowing the MH1 and MH2 domains to move freely and interact with other molecules.

This is also based on the fact that the linker of Smads is characterized by a high degree of variability in the amino acid sequence, with very few amino acid residues to be conserved among all family members (Figure 1).

Recent studies have shown that the linker region of R-Smads plays a role in the cross-talk between TGF $\beta$  and other signaling pathways. The linker is phosphorylated at specific Ser/Thr residues by MAP kinases, cyclin dependent kinases, and Ca<sup>2+</sup>/calmodulin kinase II (CaMKII) (13–19). The linker region also contains binding sites for the ubiquitin ligase Smurf1 (23). Recently, it was shown that the peptidyl-prolyl cis–trans isomerase Pin1 interacted with Smad2 and Smad3 at phosphorylated S/T-P motifs in the linker region (24). Furthermore, the linker region of Smads was shown to bind to filamin, a cytoskeletal actin-binding protein, suggesting a novel regulatory cross-talk between TGF $\beta$  signaling and the actin cytoskeleton (40). Finally, the linker regions of Smad3 and Smad4 were shown to harbor, at their C-terminal ends, a transactivation domain, and an internal deletion of this domain in Smad3 was shown to abolish Smad-mediated transactivation of TGF $\beta$  target promoters (20–22). However, naturally occurring Smad3 isoforms that lack the N-terminal part of the linker region retain their functional properties such as nuclear translocation and transcriptional activation of reporters containing SBEs (40, 41). All of the above studies support an essential role of the C-terminal part of the linker region of Smad proteins in their functions as key TGF $\beta$  signaling mediators.

**Role of Linker Amino Acids in Smad Oligomerization.** The studies described here provide additional evidence for the important role of specific amino acid residues of the linker region for Smad3-mediated signaling. One of the most intriguing findings of our present work was that substitution of the conserved amino acid glutamine 222 by alanine in the C-terminal part of the linker had a profound effect on its oligomerization with other Smad proteins and with itself (Figure 3). As a consequence, this Smad3 mutant failed to translocate to the nucleus and activate transcription in response to TGF $\beta$  stimulation (Figures 4–6). The formation of Smad oligomers in response to TGF $\beta$  stimulation is at the heart of TGF $\beta$  signaling in mammalian cells as documented by functional studies as well as by the identification of oligomerization deficient Smad mutants in cancer patients (10, 37). Smad oligomerization requires phosphorylation of R-Smads by the corresponding type I TGF $\beta$  receptor and the formation of R-Smad/Smad4 complexes in the cytoplasm (37). Crystallographic studies of Smad4 oligomerization revealed that formation of Smad trimers is facilitated by specific interactions between residues of the MH2 domain that are located in the loop-helix region and 3-helical bundle (42). We have previously characterized a tumorigenic mutation in Smad4 (E330A) and showed that this amino acid (or the corresponding residue E239 in Smad3), which is not located on the binding surface, participates in a network of polar interactions with other residues of the MH2 domain and that disruption of this network of intramolecular interactions destroys Smad oligomerization and inhibits TGF $\beta$  signaling (43). This finding, combined with our observation that residues 230–248 of the MH2 domain (which include E239) are required for the transcriptional activity of the linker, prompted us to propose that interactions between polar residues of the MH2 domain (such as E239) and the linker domain (such as Q222) contribute to the local stability of this part of the Smad3 protein and play an important role in the functions of the MH2 domain such as oligomerization. This hypothesis is

supported by our observation that the Smad3 Q222A mutant interacted less efficiently with SARA and the type I TGF $\beta$  receptor than wild type Smad3 or the other two mutants P229A and N218A (Figure 2B,C). Crystallographic studies of Smad oligomers obtained by full length proteins will be extremely valuable to help us understand the intermolecular interactions that operate between the different domains of Smads and the contribution of these interactions to Smad functionality.

Another interesting observation in our present study was that wild type Smad3 and the Smad3 mutants N218A and P229A translocated to the nucleus in Smad4-deficient MDA-MB-468 cells in response to ALK5 activation (Figure 5). This is an additional proof of the concept that activated Smad3 proteins can enter the nucleus as homo-oligomers (i.e., as homodimers or homotrimers). However, Smad3 proteins cannot enter the nucleus as monomers as shown in the case of the oligomerization-deficient Smad3 mutant Q222A (Figure 5).

Smad oligomerization is also crucial for the ability of Smads to activate transcription in the nucleus. As shown in Figure 6B, the Smad3 Q222A mutant was unable to activate transcription even when fused with the heterologous DNA binding domain of the yeast transactivator GAL4. The GAL4 DBD contains a nuclear localization signal and thus facilitates the transport of this Smad3 mutant to the nucleus (Supporting Information, Figure 1). Thus, the data of Figure 6 strongly suggested that interaction of Smad3 with other R-Smads or Smad4 in the nucleus is required not only for the cooperative binding of Smads to the DNA but also for the interaction with the basal transcription machinery and that the linker region of Smads plays a crucial role in this process.

**Enhancement of the Transactivation Potential of Smad3 by a Single Amino Acid Substitution in the Linker Region.** We show here that missense mutations at two highly conserved amino acid residues, Q222A and P229A, abolished the ability of Smad3 to transactivate a Smad-responsive promoter (CAGA<sub>12</sub>) in cooperation with Smad4 (Figure 6A). In sharp contrast, a missense mutation at a nonconserved amino acid residue, N218A, increased the transactivation potential of Smad3 (Figure 6A,B). At least two mechanisms could be proposed to account for this activating function of the N218A mutation: The N218A mutation could enhance the TGF $\beta$ -induced oligomerization of Smad3. The oligomerization assays of Figure 3, which were performed using the *in vivo* biotinylation assay, did not reveal any changes in the homo- or the hetero-oligomerization properties of the Smad3 N218A mutant when compared to the wild type protein or in the ALK5-stimulated C-terminal phosphorylation of this mutant. Although the immunofluorescence assays of Figure 4 are not sensitive enough to detect subtle changes in the nuclear accumulation between the wild type and the N218 mutant in response to ALK5 signaling, no major differences were observed. Alternatively, the N218A mutation could increase the interaction of Smad3 with coactivators in the nucleus. The possibility remains that the Smad3 N218A mutation creates a novel binding surface which enhances the interaction of Smad3 with coactivators in the nucleus.

**Amino Acid Residue P229 of the Smad3 Linker Contributes to DNA Binding.** The Smad3 P229A mutant was perhaps the most interesting of all the mutants that we generated in the context of the present study. The P229A mutation, which is localized at the very-C-terminal end of the linker (Figure 1), did not abrogate the ability of Smad3 to interact with SARA (Figure 2C), to be phosphorylated by the ALK5 receptor



(Figure 2B) and to form oligomers with other Smad molecules or with itself (Figure 3B–D). The P229A mutant translocated to the nucleus in response to ALK5 activation (Figures 4 and 5) and failed to transactivate the CAGA<sub>12</sub> reporter (Figure 6A), but it retained its transactivation potential when fused to the heterologous DNA binding domain of the yeast transactivator GAL4 (Figure 6B). These findings strongly suggested that the major defect in the Smad3 P229A mutant was in DNA binding. To address this issue, we performed protein–DNA binding assays *in vitro* and *in vivo* and indeed showed that the Smad3 protein bearing the P229A mutation had lost its capacity to interact with promoter regions bearing well characterized Smad binding elements (SBEs) such as the p21 promoter or the PAI-1 promoter (Figure 8A–C) (34, 44). As far as we know, this is the first report of linker mutation affecting the DNA binding properties of Smads. We could only speculate about the possible causes for this DNA binding defect based on the crystal structure of the transcriptionally active form of Smad4, the only solved structure containing a fragment of the linker (45). Smad4 contains a proline rich transactivation domain in the junction between the linker and the MH2 domain called the SAD (Smad4 activation domain) (22). Proline-rich transactivation domains are found in other transcription factors such as CTF (CCAAT box transcription factor)/NFI (nuclear factor I) and AP-2 (activator protein 2) (46, 47). The crystal structure of SAD revealed that it forms two well-ordered structures (residues 285–296 and 307–318) separated by a disordered region (residues 297–306) (45). Residues 307–318 in Smad4, which include E307, Q311, and P318 (the corresponding residues of N218, Q222 and P229 in Smad3), form an extended loop structure (SAD loop) that connects to the MH2 domain. Most of the hydrophobic residues of the SAD loop are solvent-exposed (45). This energetically unfavorable surface could be stabilized through hydrophobic interaction with a transcription partner. We have shown previously that a region in Smad3 that corresponds to Smad4 SAD is transcriptionally active both in mammalian cells and in yeast and that an internal deletion of this region abolished Smad3-mediated transactivation (21). Whether Smad3 forms a SAD structure similar to Smad4 is not presently known, but we are tempted to speculate that mutation P229 in Smad3 prevents interaction with a nuclear cofactor which helps to tether Smad3 to the DNA. An alternative possibility is that P229 participates in hydrophobic interactions with nonpolar residues in the MH1 domain, thus stabilizing the  $\beta$ -hairpin structure which makes contacts with the Smad binding elements, but this needs to be investigated further by structural studies.

**Dominant Negative Function of the Smad3 P229A Mutant.** Finally, the Smad3 P229A mutant had a potent dominant negative effect on TGF $\beta$  signaling (Figure 7). Of note was the strong inhibitory effect of P229A mutant on Smad4-mediated transactivation (Figure 7B and C). This observation combined with the finding that Smad3 P229A interacted with Smad4 in a CA-ALK5-dependent manner *in vivo*, suggested that Smad3 P229A squelches endogenous Smad4 by preventing its oligomerization with endogenous wild type Smad3 or Smad2 and as a consequence the transcriptional activation of TGF $\beta$  target genes. Alternatively, overexpressed Smad3 P229A could squelch coactivators that are required for the Smad-mediated transactivation of TGF $\beta$  target genes.

In summary, the findings of the present study indicate that amino acid residues that are located within the linker region of Smad3 play various roles in Smad functions such as oligomer-

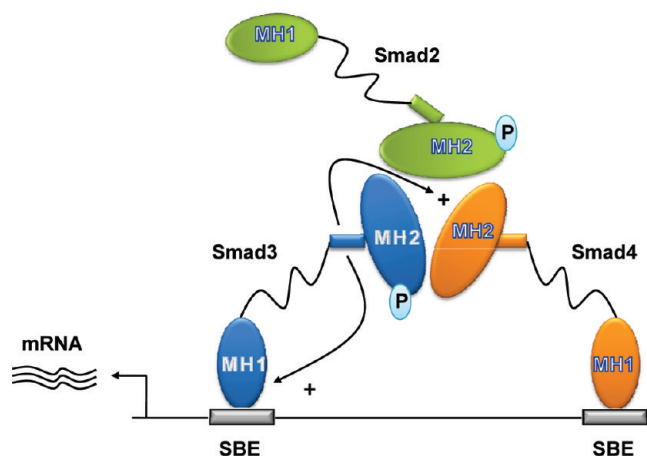


FIGURE 9: Role of the linker domain in Smad oligomerization, DNA binding, and transcriptional activation. The oligomerization of Smads leading to the formation of trimeric R-Smad/Smad4 complexes is shown using different colors for each Smad subunit. The MH1 and MH2 domains are represented by ovals, and the C-terminal region of the linker domain is represented by rectangles. The arrows emphasize the contribution of this region to Smad oligomerization and DNA binding. SBE: smad binding element.

ization and DNA binding in response to TGF $\beta$  stimulation. This is illustrated in Figure 9. Our data are in line with previous studies supporting that the linker is not just a flexible hinge that allows the MH1 and MH2 domains to move freely and interact with other molecules but plays an important regulatory role in Smad functions as key mediators of TGF $\beta$  signal transduction in mammalian cells.

## ACKNOWLEDGMENT

We thank all members of the Kardassis lab for useful discussions and suggestions and Dr. Aris Moustakas for commenting on the manuscript. E.V. and K.S.S. are graduate students of the interdepartmental graduate program in Molecular Biology-Biochemistry and S.M. is a graduate student of the graduate program in Molecular Basis of Human Disease of the University of Crete Medical School.

## SUPPORTING INFORMATION AVAILABLE

Immunofluorescence experiment using the anti-Smad3 monoclonal antibody followed by a secondary anti-mouse Alexa Fluor antibody. This material is available free of charge via the Internet at <http://pubs.acs.org>.

## REFERENCES

- Massague, J. (1998) TGF-beta signal transduction. *Annu. Rev. Biochem.* 67, 753–791.
- Sporn, M. B., and Roberts, A. B. (1992) Transforming growth factor-beta: recent progress and new challenges. *J. Cell Biol.* 119, 1017–1021.
- Massague, J., and Gomis, R. R. (2006) The logic of TGFbeta signaling. *FEBS letters* 580, 2811–2820.
- Siegel, P. M., and Massague, J. (2003) Cytostatic and apoptotic actions of TGF-beta in homeostasis and cancer. *Nature Rev.* 3, 807–821.
- Shi, Y., and Massague, J. (2003) Mechanisms of TGF-beta signaling from cell membrane to the nucleus. *Cell* 113, 685–700.
- Moustakas, A., Souchelnytskyi, S., and Heldin, C. H. (2001) Smad regulation in TGF-beta signal transduction. *J. Cell Sci.* 114, 4359–4369.
- Massague, J., Seoane, J., and Wotton, D. (2005) Smad transcription factors. *Genes Dev.* 19, 2783–2810.

8. Shi, Y., Wang, Y. F., Jayaraman, L., Yang, H., Massague, J., and Pavletich, N. P. (1998) Crystal structure of a Smad MH1 domain bound to DNA: insights on DNA binding in TGF-beta signaling. *Cell* 94, 585–594.
9. Kurisaki, A., Kose, S., Yoneda, Y., Heldin, C. H., and Moustakas, A. (2001) Transforming growth factor-beta induces nuclear import of Smad3 in an importin-beta1 and Ran-dependent manner. *Mol. Biol. Cell* 12, 1079–1091.
10. Shi, Y., Hata, A., Lo, R. S., Massague, J., and Pavletich, N. P. (1997) A structural basis for mutational inactivation of the tumour suppressor Smad4. *Nature* 388, 87–93.
11. Massague, J. (2008) TGFbeta in Cancer. *Cell* 134, 215–230.
12. Hata, A., Shi, Y., and Massague, J. (1998) TGF-beta signaling and cancer: structural and functional consequences of mutations in Smads. *Mol. Med. Today* 4, 257–262.
13. Massague, J. (2003) Integration of Smad and MAPK pathways: a link and a linker revisited. *Genes Dev.* 17, 2993–2997.
14. Mulder, K. M. (2000) Role of Ras and Mapks in TGFbeta signaling. *Cytokine Growth Factor Rev.* 11, 23–35.
15. Kretzschmar, M., Doody, J., and Massague, J. (1997) Opposing BMP and EGF signalling pathways converge on the TGF-beta family mediator Smad1. *Nature* 389, 618–622.
16. Kretzschmar, M., Doody, J., Timokhina, I., and Massague, J. (1999) A mechanism of repression of TGFbeta/Smad signaling by oncogenic Ras. *Genes Dev.* 13, 804–816.
17. Liu, F. (2006) Smad3 phosphorylation by cyclin-dependent kinases. *Cytokine Growth Factor Rev.* 17, 9–17.
18. Liu, F., and Matsuura, I. (2005) Inhibition of Smad antiproliferative function by CDK phosphorylation. *Cell Cycle* 4, 63–66.
19. Wicks, S. J., Lui, S., Abdel-Wahab, N., Mason, R. M., and Chantry, A. (2000) Inactivation of smad-transforming growth factor beta signaling by Ca(2+)-calmodulin-dependent protein kinase II. *Mol. and Cell. Biol.* 20, 8103–8111.
20. Wang, G., Long, J., Matsuura, I., He, D., and Liu, F. (2005) The Smad3 linker region contains a transcriptional activation domain. *Biochem. J.* 386, 29–34.
21. Prokova, V., Mavridou, S., Papakosta, P., and Kardassis, D. (2005) Characterization of a novel transcriptionally active domain in the transforming growth factor beta-regulated Smad3 protein. *Nucleic Acids Res.* 33, 3708–3721.
22. de Caestecker, M. P., Yahata, T., Wang, D., Parks, W. T., Huang, S., Hill, C. S., Shioda, T., Roberts, A. B., and Lechleider, R. J. (2000) The Smad4 activation domain (SAD) is a proline-rich, p300-dependent transcriptional activation domain. *J. Biol. Chem.* 275, 2115–2122.
23. Sangadala, S., Metpally, R. P., and Reddy, B. V. (2007) Molecular interaction between Smurf1 WW2 domain and PPXY motifs of Smad1, Smad5, and Smad6—modeling and analysis. *J. Biomol. Struct. Dyn.* 25, 11–23.
24. Nakano, A., Koinuma, D., Miyazawa, K., Uchida, T., Saitoh, M., Kawabata, M., Hanai, J. I., Akiyama, H., Abe, M., Miyazono, K., Matsumoto, T., and Imamura, T. (2009) Pin1 downregulates TGF-beta signaling by inducing degradation of Smad proteins. *J. Biol. Chem.* [Online early access], DOI: 10.1074/jbc.M804659-200.
25. Ho, S. N., Hunt, H. D., Horton, R. M., Pullen, J. K., and Pease, L. R. (1989) Site-directed mutagenesis by overlap extension using the polymerase chain reaction. *Gene* 77, 51–59.
26. He, T. C., Zhou, S., da Costa, L. T., Yu, J., Kinzler, K. W., and Vogelstein, B. (1998) A simplified system for generating recombinant adenoviruses. *Proc. Natl. Acad. Sci. U.S.A.* 95, 2509–2514.
27. Koutsodontis, G., and Kardassis, D. (2004) Inhibition of p53-mediated transcriptional responses by mithramycin A. *Oncogene* 23, 9190–9200.
28. Piek, E., Moustakas, A., Kurisaki, A., Heldin, C. H., and ten Dijke, P. (1999) TGF-(beta) type I receptor/ALK-5 and Smad proteins mediate epithelial to mesenchymal transdifferentiation in NMuMG breast epithelial cells. *J. Cell Sci.* 112 (Pt 24), 4557–4568.
29. Kurisaki, K., Kurisaki, A., Valcourt, U., Terentiev, A. A., Pardali, K., Ten Dijke, P., Heldin, C. H., Ericsson, J., and Moustakas, A. (2003) Nuclear factor YY1 inhibits transforming growth factor beta- and bone morphogenetic protein-induced cell differentiation. *Mol. and Cell. Biol.* 23, 4494–4510.
30. Thymiakou, E., Zannis, V. I., and Kardassis, D. (2007) Physical and functional interactions between liver X receptor/retinoid X receptor and Sple1 modulate the transcriptional induction of the human ATP binding cassette transporter A1 gene by oxysterols and retinoids. *Biochemistry* 46, 11473–11483.
31. Matsuura, I., Wang, G., He, D., and Liu, F. (2005) Identification and characterization of ERK MAP kinase phosphorylation sites in Smad3. *Biochemistry* 44, 12546–12553.
32. Zhu, H., Kavsak, P., Abdollah, S., Wrana, J. L., and Thomsen, G. H. (1999) A SMAD ubiquitin ligase targets the BMP pathway and affects embryonic pattern formation. *Nature* 400, 687–693.
33. Rodriguez, P., Braun, H., Kolodziej, K. E., de Boer, E., Campbell, J., Bonte, E., Grosveld, F., Philipsen, S., and Strouboulis, J. (2006) Isolation of transcription factor complexes by in vivo biotinylation tagging and direct binding to streptavidin beads. *Methods Mol. Biol.* 338, 305–323.
34. Dennler, S., Itoh, S., Vivien, D., ten Dijke, P., Huet, S., and Gauthier, J. M. (1998) Direct binding of Smad3 and Smad4 to critical TGF beta-inducible elements in the promoter of human plasminogen activator inhibitor-type 1 gene. *EMBO J.* 17, 3091–3100.
35. Tsukazaki, T., Chiang, T. A., Davison, A. F., Attisano, L., and Wrana, J. L. (1998) SARA, a FYVE domain protein that recruits Smad2 to the TGFbeta receptor. *Cell* 95, 779–791.
36. Qin, B. Y., Lam, S. S., Correia, J. J., and Lin, K. (2002) Smad3 allosterically links TGF-beta receptor kinase activation to transcriptional control. *Genes Dev.* 16, 1950–1963.
37. Moustakas, A., and Heldin, C. H. (2002) From mono- to oligo-Smads: the heart of the matter in TGF-beta signal transduction. *Genes Dev.* 16, 1867–1871.
38. de Winter, J. P., Roelen, B. A., ten Dijke, P., van der Burg, B., and van den Eijnden-van Raaij, A. J. (1997) DPC4 (SMAD4) mediates transforming growth factor-beta1 (TGF-beta1) induced growth inhibition and transcriptional response in breast tumour cells. *Oncogene* 14, 1891–1899.
39. Stroschein, S. L., Wang, W., and Luo, K. (1999) Cooperative binding of Smad proteins to two adjacent DNA elements in the plasminogen activator inhibitor-1 promoter mediates transforming growth factor beta-induced smad-dependent transcriptional activation. *J. Biol. Chem.* 274, 9431–9441.
40. Sasaki, A., Masuda, Y., Ohta, Y., Ikeda, K., and Watanabe, K. (2001) Filamin associates with Smads and regulates transforming growth factor-beta signaling. *J. Biol. Chem.* 276, 17871–17877.
41. Kjellman, C., Honeth, G., Jarnum, S., Lindvall, M., Darabi, A., Nilsson, I., Edvardsen, K., Salford, L. G., and Widegren, B. (2004) Identification and characterization of a human smad3 splicing variant lacking part of the linker region. *Gene* 327, 141–152.
42. Shi, Y. (2001) Structural insights on Smad function in TGFbeta signaling. *BioEssays* 23, 223–232.
43. Prokova, V., Mavridou, S., Papakosta, P., Petratos, K., and Kardassis, D. (2007) Novel mutations in Smad proteins that inhibit signaling by the transforming growth factor beta in mammalian cells. *Biochemistry* 46, 13775–13786.
44. Seoane, J., Le, H. V., Shen, L., Anderson, S. A., and Massague, J. (2004) Integration of Smad and forkhead pathways in the control of neuroepithelial and glioblastoma cell proliferation. *Cell* 117, 211–223.
45. Qin, B., Lam, S. S., and Lin, K. (1999) Crystal structure of a transcriptionally active Smad4 fragment. *Structure* 7, 1493–1503.
46. Kim, T. K., and Roeder, R. G. (1993) Transcriptional activation in yeast by the proline-rich activation domain of human CTF1. *J. Biol. Chem.* 268, 20866–20869.
47. Williams, T., and Tjian, R. (1991) Analysis of the DNA-binding and activation properties of the human transcription factor AP-2. *Genes Dev.* 5, 670–682.